We are IntechOpen, the world's leading publisher of Open Access books Built by scientists, for scientists

6,900
Open access books available

185,000
International authors and editors

200M
Downloads

Our authors are among the

154
Countries delivered to

TOP 1%
most cited scientists

12.2%
Contributors from top 500 universities

CLARIVATE ANALYTICS
BOOK CITATION INDEX
INDEXED

WEB OF SCIENCE™

Selection of our books indexed in the Book Citation Index
in Web of Science™ Core Collection (BKCI)

Interested in publishing with us?
Contact book.department@intechopen.com

Natural Gas Treatment Using Adsorptive Separation

Pramathesh R. Mhaskar and Arun S. Moharir

Additional information is available at the end of the chapter

1. Introduction

Natural Gas (NG) is used both as a process gas as well as a fuel. The two uses make contrary demands on its composition. Natural Gas is a mixture of Methane(C_1), Ethane (C_2), Propane (C_3), Butane isomers (C_4) and Pentanes, to name only the more significant components. It can have Carbon-Dioxide, Hexanes etc. as other components. Higher hydrocarbons are there as the gas comes off the well, but are removed in the gas treatment plants. Similarly, water, if any, is removed. Winterization and dehydration are two major aspects of gas treatment before it is transported to the user through pipelines [1].

When the use of Natural Gas is as a fuel replacing conventional sources such as coal, or furnace oil or petroleum fractions, the most important thing is its calorific value. Higher the content of higher hydrocarbons, higher is the calorific value of the feed gas. Natural Gas is predominantly Methane with second most abundant component being Ethane. C_{2+} alkanes (Propane and higher alkanes) together are about 4 or less %. Even this small percentage of higher hydrocarbons can change the calorific value significantly. For example, pure Methane has a lower calorific value of 850 kJ/mole, while a mixture of 97% Methane and 3% n-Butane has a lower calorific value of 904 kJ/mole. Users of Natural Gas as fuel thus would like more presence of the heavier hydrocarbons in the supply gas.

Gas based fertilizer plants, metallurgical units which need to carry out ore reduction using gases such as CO and H_2 would like to use Natural Gas as mainly a feedstock for reformers. Even a small presence of C_{2+} could be detrimental to the reformer catalyst and necessitate its regeneration frequently. Natural Gas is thus necessarily stripped of its C_{2+} content before use as reformer feedstock. One of the techniques used is cooling the gas below the boiling points of Propane so that C_{2+} hydrocarbons are condensed. Joule-Thompson expansion is often employed to achieve temperatures as low as 203 K for this purpose. This leaves a mixture predominantly of C_1 and C_2 for reforming. C_{2+} alkanes are recovered almost entirely and can

contribute to Liquefied Petroleum Gas (LPG) pool. Turbo expansion is a costly technology, both in terms of capital and operating cost. An alternative separation technique is desired for large scale gas treatment for removal of C_{2+} from Natural Gas.

This paper deals with an adsorption based technique developed and implemented for this purpose. Pressure Swing Adsorption (PSA) was used as an alternative. Due the large volume that needed to be treated, we could conceive a significant modification in PSA technology. By suitable application of model based design and operation, we could convert the PSA to a surge-less PSA technology. This eliminated or minimized the need for surge vessels, so integral to any PSA process because of pressure swings. The job of surge tanks was sought to be done by appropriate pressure/flow control of feed to and product from the adsorption beds. This paper discusses the conceptual design process design and process plant engineering of a surge-less PSA plant designed to process a feed rate as high as 2000000 m^3 per day of Natural Gas at standard temperature and pressure conditions. This makes it one of the largest functional adsorptive separation units.

1.1. Design problem

The separation plant's objective was to reduce C_{2+} content of Natural Gas to below 0.6% (mole fraction) for all feed compositions with C_{2+} content not exceeding 2%. It was even this relatively low content of C_{2+} hydrocarbons which was perceived to be causing catalyst deactivation due to coking in downstream reactors.

The main components of the Natural Gas are given in Table 1 and a typical feed gas composition used in design was as given in Table 2. The operating temperature was the ambient value at site equal to 303.15 K. The viscosity of the feed gas at this temperature was 0.000012 Pa-s. This value was used to estimate the pressure drop across the bed.

i	Component Formula	b_i (m³/mole)	q_i^{max} (moles adsorbed/ m³ particles)
1	C_3H_8	0.008400	9091
2	$n\text{-}C_4H_{10}$	0.014970	12771
3	$i\text{-}C_4H_{10}$	0.019770	8019
4	CO_2	0.006400	9470
5	C_2H_6	0.002500	9009
6	CH_4	0.000550	7812

Table 1. Fitted values of pure component Langmuir adsorption isotherm parameters on Silica Gel at 303.15 K temperature

Component	y_i	Molecular Weight (g/mole)	w_i	b_i (m³/mole)	q_{max} (moles adsorbed/m³ particles)	q_i^* at total pressures of 1 bara and 34 bara respectively (moles adsorbed/m³ particles)
Propane	0.0065	44	0.0171	0.00840	7925.4	16.7 and 296.9
n-Butane	0.0011	58	0.0038	0.01497	7925.4	5.0 and 89.6
i-Butane	0.0010	58	0.0035	0.01977	7925.4	6.0 and 107.5
Carbon Dioxide	0.0074	44	0.0194	0.00640	7925.4	14.5 and 257.6
Ethane	0.0188	30	0.0337	0.00250	7925.4	14.4 and 255.6
Methane	0.9652	16	0.9225	0.00055	7925.4	162.3 and 2886.9

Table 2. Adsorption capacity of each component of the NG mixture as per Extended Langmuir isotherm at 303.15 K temperature (Case 1: no component lumping)

The hydrocarbons as well as CO_2 are adsorbed by several adsorbent materials. Most important among them are Activated Carbon and Silica Gel [1]. Silica Gel was the adsorbent material considered in this work. Limited data on adsorption thermodynamics is available in terms of adsorption isotherms [2]. The adsorption capacities increase significantly with increase in the number of Carbon atoms in the homologous series of alkanes of interest, namely C_1 to C_4. Typical pure-component isotherms at the operating temperature and pressures up to 35 bara and the parameters of the fitted curves for the five hydrocarbons are shown in Figure 1 and Table 1 respectively. Carbon Dioxide has also been reported for its adsorption behavior and its isotherm and isotherm expressions are also included in Figure 1 and Table 1. The isotherms show typical favorable isotherm shape and fit very well with Langmuir equation.

The isotherms and their mathematical expression forms show the adsorption equilibrium constant increasing with the number of Carbon atoms in the alkane molecule. The mathematical expressions can be used to appreciate the separation potential offered by Silica Gel for the desired separation task. If the Natural Gas composition given above is equilibrated with Silica Gel, the equilibrium adsorbed phase concentration of each of the six components is tabulated in Table 2 based on Extended Langmuir expression for multi-component adsorption. The pressure of gas was taken as 1 bara in this calculation. If the Natural Gas is available at higher pressure, the selectivities can be even better. For example, the feed gas pressure for the design case was 34 bara. If the feed composition is the same, but equilibration is done at 34 bara, the equilibrium adsorbed phase concentration of each component is also tabulated in Table 2. Higher pressures do not seem to help as the saturation capacities are reached. Physical adsorption being reasonably weak, multi-layer adsorption is less possible and monolayer saturation capacities are reached at the pressures

considered. At both pressures, the solid phase has considerable amount of adsorbed CH_4 (74% on molar basis or 52% on mass basis of adsorbed phase is Methane). It is the major component of the adsorbed phase as its mole fraction in the feed itself exceeds 95%. So significant amounts of this adsorbed Methane will be lost during the depressurization step.
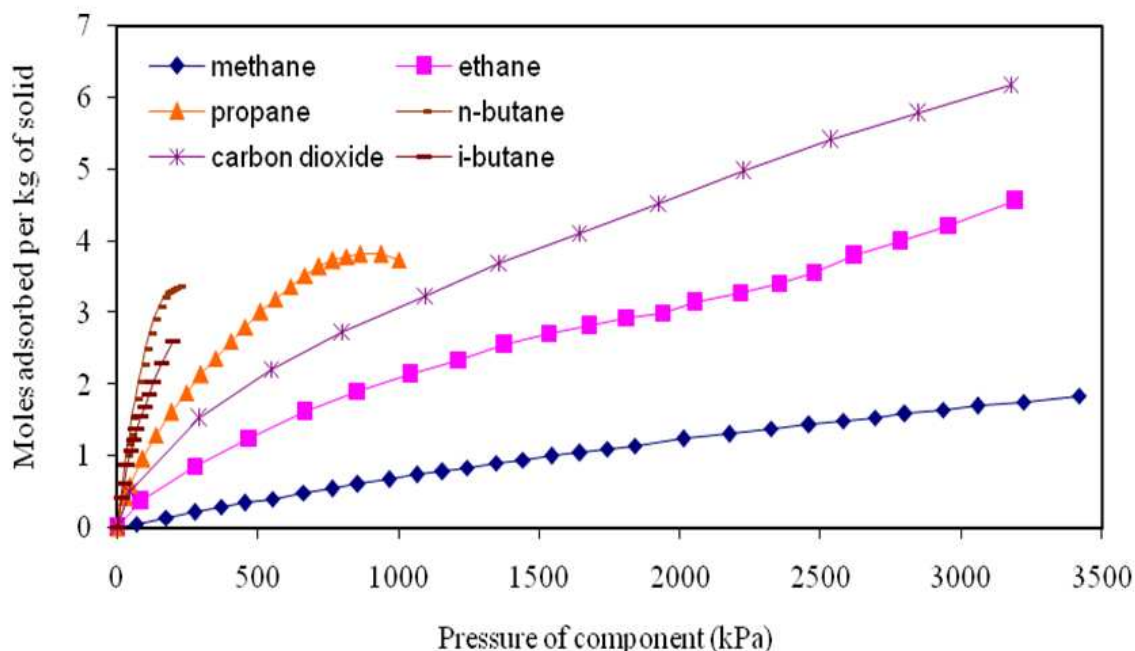

Figure 1. Pure component adsorption isotherms on Silica Gel at 303.15 K

These preliminary adsorbent evaluation studies indicated suitability of Silica Gel as a suitable adsorbent. If a bed of Silica Gel is subjected to a flow of Natural Gas, the simultaneous adsorption of the hydrocarbons and CO_2 will occur. The concentrations of higher hydrocarbons (due to their lower value and stronger preference by the adsorbent) would deplete fast and one can expect a raffinate gas leaner in the C_{2+} content.

The bed would get gradually saturated and C_{2+} gases would begin to break through into the raffinate. If the feed gas is then diverted to another identical bed and the saturated bed is regenerated, continuous raffinate production is possible. Regeneration can be carried out by depressurization of the bed. The desorption of C_{2+} can also be facilitated by passing through the bed a fraction of the lean gas (LG) produced earlier or purge-in gas (PG) which will reduce the partial pressure of C_{2+} components in the bulk phase surrounding the adsorbent particles. This would help effect further regeneration and carry away of the desorbed component. The gas collected during these blow down and purging steps will be richer in C_{2+} components than the feed gas and is termed as rich gas (RG). The adsorbed bed switched between alternate high and low pressure regimes thus offer a potential to separate the Natural Gas into two streams, namely a raffinate leaner in C_{2+} than the feed and an extract gas richer in C_{2+} components. We thus have a potential to employ a suitably designed PSA process for the desired separation task.

The design was carried out using a comprehensive simulation model for PSA processes developed by the authors [3]. These simulation studies and their findings in terms of an optimal PSA cycle is discussed in the next sections.

1.2. Cycle description

Refer to Figure 2 and Table 3. The description of the symbols in Figure 2 is given in the nomenclature section. In Natural Gas-Silica Gel system, the desired product is the weakly adsorbed component (Methane and Ethane). This is the characteristic feature of raffinate PSA systems. Conventional 4-step cycle of the Skarstrom type is used for dealing with raffinate PSA systems [4]. The steps of the Skarstrom cycle in sequence are: pressurization of the bed with feed gas to the feed tank pressure which is the adsorption pressure, adsorption of feed gas at the adsorption pressure to give raffinate product, depressurization of the bed to the desorption pressure in a direction counter-current to that of the feed gas flow direction and counter-current purge with fraction of raffinate product at the desorption pressure.
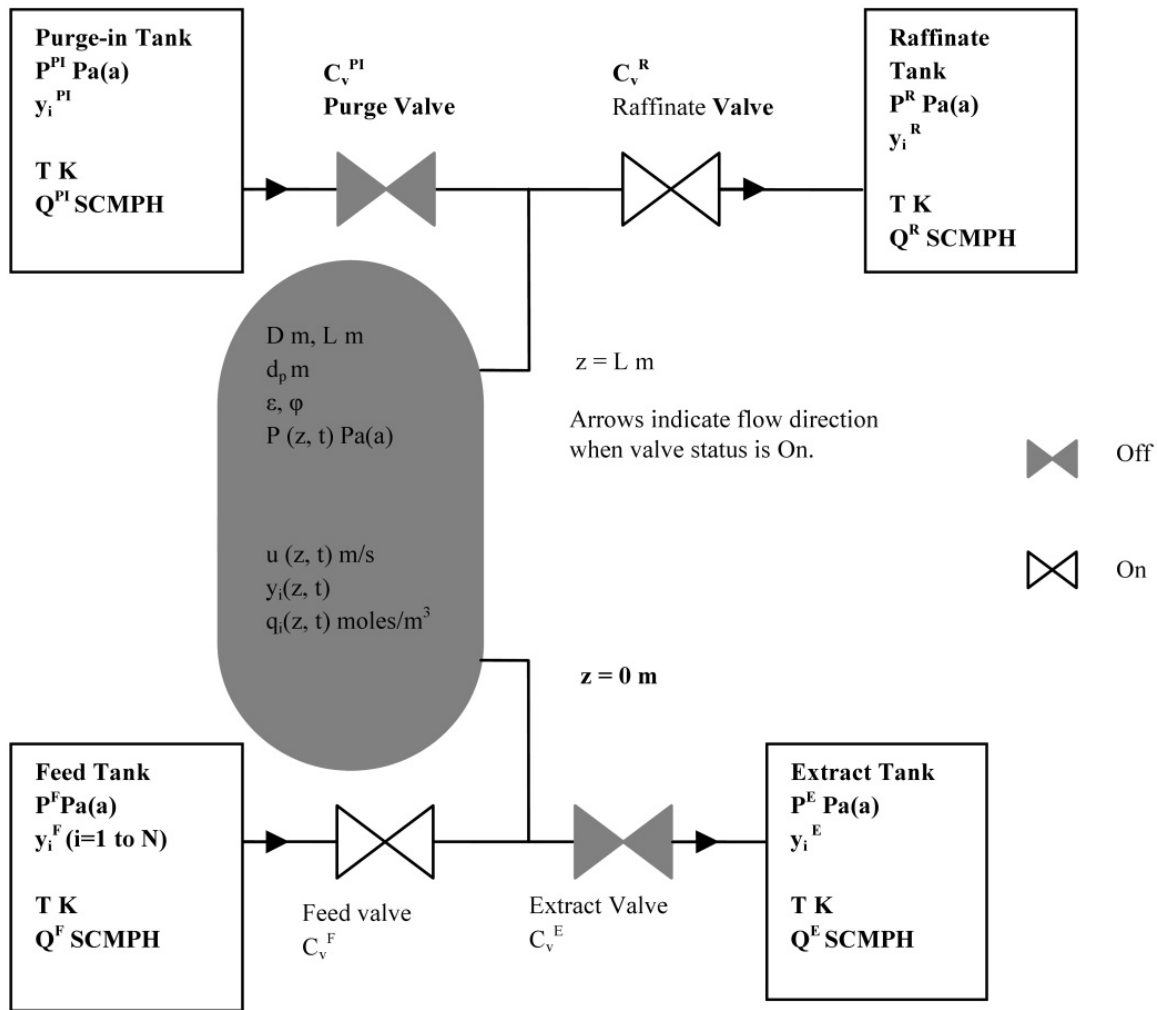

Figure 2. State of a bed in feed adsorption step

Step	Description	Feed valve	Raffinate valve	Extract valve	Purge valve
1	Feed pressurization	On	Off	Off	Off
2	Feed adsorption	On	On	Off	Off
3	Co-current depressurization to raffinate tank	Off	On	Off	Off
4	Counter-current depressurization to extract tank	Off	Off	On	Off
5	Counter-current purge by fraction of raffinate	Off	Off	On	On

Table 3. Steps, their sequence and the valve status for PSA cycle for Natural Gas treatment

In this work, an additional step of depressurization is added after adsorption step and before the counter-current depressurization step, thus creating a 5-step cycle. Stepwise description of the PSA cycle used in the current work is as follows:

Step 1: Feed pressurization (duration = t_1 seconds)

The bed pressure is much lower than the feed tank pressure. The valve connecting the feed tank to the bed is opened. The other valves are closed. The bed starts getting pressurized with the feed Natural Gas mixture and at the end of this step, the bed is pressurized to a value nearly equal to the feed tank pressure. Simultaneous adsorption/desorption that takes place, is considered in the PSA process model.

Step 2: Feed adsorption (duration = t_2 seconds)

The valve connecting the raffinate tank to the bed is opened at the start of this step. Since the raffinate tank pressure is less than that of the pressurized bed, material starts flowing out from the bed to the raffinate tank and fresh feed flows into the bed. The raffinate tank collects a gas that is relatively free of Propane and higher alkanes and Carbon Dioxide as these components get preferentially adsorbed in the adsorbent. Pressure in the bed remains reasonably constant in this step except developing small pressure drop across the bed due to flow.

Step 3: Co-current depressurization to Raffinate tank (duration = t_3 seconds)

At the start of this step, the feed tank connection is closed and the weaker adsorbates that may be trapped in the void space of the bed are released into the raffinate tank. Desorption of the species will also occur simultaneously with depressurization and the model considers it. This step is included to improve the recovery of the weaker adsorbates and reduce the velocity surges that would have occurred in Step 4 if the bed is directly depressurized counter-currently to the extract tank after finishing the adsorption step. This step also increases the chance of getting an extract more pure in the stronger adsorbate[3].

Step 4: Counter-current depressurization to Extract tank (duration = t_4 seconds)

At the start of this step, the raffinate tank connection is closed and the extract tank connection is opened. The extract tank is at a much lower pressure than the bed pressure. The bed starts depressurizing counter-currently. Desorption of heavier species takes place as the pressure decreases. The desorbed gas is collected in the extract tank.

Step 5: Counter-current purge with fraction of the raffinate (duration = t_5 seconds)

Some fraction from the raffinate tank is used for purging counter-currently the already depressurized bed. In the model, a separate purge-in tank is shown as supplying this purge gas. Its composition is set internally as the same as raffinate composition. The purge-in tank is at a higher pressure than the depressurized bed. The valve connecting the purge-in tank to the bed is opened at the start of this step. The purge gas enters the bed and starts flowing counter-currently through the bed. This step is used to flush the desorbed heavy components in the void spaces towards the extract end. The outgoing stream from this step is also collected in the extract tank. One cycle is completed at the end of this step (at $t_1+t_2+t_3+t_4+t_5 = t_{cycle}$) and a fresh cycle begins starting with Step 1.

2. Simulation model

PSA is a very versatile process and the process embodiments most suited for a given separation task depend entirely on the adsorbent-adsorbate system and desired separation performance. Optimal design and operation alone can help achieve the best out of this technology. To study various process options, an elaborate and costly experimental program needs to be launched and executed. Another equally effective, much less costlier and more exhaustive option that is possible is to systematically carry out simulation based design. A rigorous and predictive model of the process physics is at the core of this approach. The authors have developed a generic simulator for PSA process genre covering all its possible variations such as PSA, Vacuum Swing Adsorption (VSA), Pressure-Vacuum Swing Adsorption (PVSA), etc. The model allows putting together any PSA cycle and predict its effect on performance measured in terms of product purity, recovery and adsorbent throughput. The model has been presented in detail elsewhere [3]. A relevant summary along with the definitions of performance indices for the present case is presented here.

The model mainly assumes-(i) perfectly plug flow of the fluid, (ii) fluid behaves like an ideal gas, (iii) multi-component adsorption equilibrium behavior as per Extended Langmuir isotherm, (iv) isothermal operation, (v) mass transfer rate described by the linear driving force approximation model, (vi) flow at the ends of the bed described by a valve equation with the ability to vary the valve coefficient with respect to time in case of controlled opening or closing of the valve and (vii) pressure drop across the packed bed is described by the Ergun equation. The model can consider- (i) sorption occurs during the pressurization and depressurization steps (no frozen solid assumption), (ii) fluid velocity variations, (iii) fluid density variations and (iv) presence of inert or empty layer below or above the adsorbent layer. Equations (1)-(7) are the main equations of the model and are given in Table 4.

Overall mole balance for ith component

$$\frac{\partial(uc_i)}{\partial z} + \varepsilon\frac{\partial c_i}{\partial t} + (1-\varepsilon)\frac{\partial q_i}{\partial t} = 0 \qquad i = 1, 2, .., N \qquad (1)$$

Extended Langmuir isotherm

$$\frac{q_i^*}{q^{max}} = \frac{b_i c_i}{1 + \sum\limits_{j=1}^{N}(b_j c_j)} \qquad i = 1, 2, .., N \qquad (2)$$

Linear Driving Force Approximation model for mass transfer

$$\frac{\partial q_i}{\partial t} = k_i^{LDF}(q_i^* - q_i) \qquad i = 1, 2, .., N \qquad (3)$$

Ideal gas law

$$c_i = \frac{P y_i}{RT} \qquad i = 1, 2, .., N \qquad (4)$$

Ergun equation for pressure drop

$$\frac{-\partial P}{\partial z} = 150\frac{\mu(1-\varepsilon)^2 u}{g_c \phi^2 d_p^2 \varepsilon^3} + 1.75\frac{(1-\varepsilon)u^2 \varrho}{g_c d_p \phi \varepsilon^3} \qquad (5)$$

Valve equation to get velocity at the bed end where valve is open

$$u = C_v \frac{\sqrt{P^{US} - P^{DS}}}{\sqrt{\varrho}} \qquad (6)$$

Stoichiometric condition in fluid phase

$$\sum\limits_{i=1}^{N} y_i = 1 \qquad (7)$$

Model performance parameters
Recovery of Propane and heavier alkanes

$$\%\,Recovery = 100\,\frac{\int\limits_{t=t_1+t_2+t_3}^{t=t_{cycle}}(uPy_{UD})_{z=0}^t dt}{\int\limits_{t=0}^{t=t_1+t_2}(uPy_{UD})_{z=0}^t dt} \qquad (8)$$

Purity of Methane and Ethane in raffinate

$$\%\,Purity = 100\,\frac{\int\limits_{t=t_1}^{t=t_1+t_2+t_3}(uP(1-y_{UD}))_{z=L}^t dt}{\int\limits_{t=t_1}^{t=t_1+t_2+t_3}(uP)_{z=L}^t dt} \qquad (9)$$

Table 4. Important model equations and performance indices

The model performance parameters for given design and operating conditions used in this work are given by Equations (8) and (9) in Table 4. (See the nomenclature section for a description of the symbols in Table 4.)

1) Although getting a raffinate free of heavier hydrocarbons (C_3 and above) was an objective of this PSA, the same heavier components were also desired to be recovered to as high an extent as possible as they serve as LPG components. Recovery in this case is therefore defined as the percentage of these components from the feed gas which end up in the extract stream over a complete cycle. The definition is as in Equation (8). y_{UD} is the summation of mole fractions of all undesirable components in the raffinate, for example, the heavier hydrocarbons and CO_2.

2) The raffinate is considered as 100% pure if does not contain these heavy components (C_3 and above) and CO_2. Purity is therefore defined as the difference between 100 and mole percent of these undesirable components in the raffinate over a complete cycle. The definition is given as Equation (9).

3) Additionally, the feed rate was the average hourly volumetric flow rate of Natural Gas to a single bed in a complete cycle at Standard Temperature and Pressure conditions. This was also a performance parameter. It was estimated from the total moles of Natural Gas fed in a cycle to a bed and the cycles completed in an hour.

The mass balance equations in the form of differential algebraic equation (DAE) are discretized using finite difference technique. This converts the model equations into a set of simultaneous algebraic equations, which relate all the variables at an advanced time step to their values at the immediately previous time interval (initial conditions). A marching solution can thus be launched to model the bed performance during each step. Pressure and flow velocity, bulk and adsorbed phase concentrations for all the components at all grid points along the bed become the algebraic variables. For each step of the cycle, the boundary conditions as above are then specifications of relevant variables at the bed ends. After discretization and applying suitable boundary conditions, the number of variables becomes equal to the number of equations. Thus, degrees of freedom become zero. The number of such variables in each step of the cycle depend upon the number of divisions the bed is discretized into, and the number of components as given in Table 5.

Then the variables were normalized and non-dimensionalized. An upwind implicit scheme is used for the spatial discretization and a backward difference scheme is used for the temporal discretization. Both the schemes were of first order accuracy but simple and unconditionally stable. Discretization results in a system of simultaneous non-linear algebraic equations linking the variable values at an advanced time increment to the values at immediately previous time increment. The generation of the set of equations and its solution is repeated to march in time. Convergent temporal and spatial grid sizes were found by successively reducing them and simulating the cyclic steady state till differences in the concentration profiles vanished signifying convergence. Grid size reduction also helped in improvement in mass balance closures.

Step of the cycle	Number of variables (equations)	Remarks
Adsorption, purge and rinse	2+N+M(2N+2)	
Pressurization and depressurization	1+N+M(2N+2)	
Idle	N+M(2N+2)	Lowest no. of variables
Pressure equalization	N+(2M+1)(2N+2)	Highest no. of variables

Table 5. Number of variables for each step of the cycle as a function of number of components (N) and number of divisions (M) used for spatial discretization

The system of simultaneous non-linear algebraic equations is solved by using Powell's hybrid method. It is implemented in Fortran programming language. Initial guess for each unknown variable, maximum number of iterations, step size for Jacobian evaluation and tolerance have to be provided by the user. Powell's method is a combination of Newton's method and the steepest descent method and offers improved convergence as compared to Newton's method. As we march from one time step to another, the known conditions at the current time are provided as the initial guess for the respective unknowns of the advanced time step. The solver returns the converged solution with the stipulated accuracy. These values are used as the initial guess for the unknowns of the next time step and so on. The system of non-linear algebraic equations is converted to linear ones by estimating the Jacobian based on a finite difference approximation. The inverse of the Jacobian is calculated and used for giving the improved solution.

At start-up, the bed is assumed to be at the pressure of extract tank and contains pure CH_4 (most weakly adsorbed component) in both the phases. For simulation with component lumping, the bed is assumed to be filled with the pseudo-component having the lowest adsorption equilibrium constant. The adsorbed phase and the bulk phase are assumed to be in adsorption equilibrium at this pressure. After the first cycle, the initial conditions of the bed are the conditions of the bed at the end of the last step of the first cycle. Similarly, the initial conditions for any step are the conditions at the end of the previous step in the cycle. Each step is uniquely described by a boundary condition on velocity and the inlet fluid stream composition.

The PSA steps are simulated in a given sequence to simulate a PSA cycle. As the PSA cycles are simulated iteratively, a cyclic steady state (CSS) is achieved where the spatial-temporal concentration profiles of each component in each phase as well as the pressure and the velocity profiles in the bed during and at the end of each step in a cycle match the corresponding profiles in the corresponding step in the immediately previous cycle within the tolerance limit. This is the simulated cyclic steady state performance, which could then be evaluated analytically in terms of derived performance parameters such as product purity, recovery, and adsorbent throughput etc.

When the cyclic steady state is achieved, the time series of bulk phase concentrations and velocities entering and leaving the bed provide the transient detail of inputs to and outputs from the PSA system. Suitable numerical integration of these instantaneous profiles with respect to time at each of the bed ends summarize the input and output molar flows of all feed and product streams respectively over each step of a PSA cycle (integration limits are over the step duration). The PSA cycle configuration in terms of step durations used with this gives the net hourly input-output flow rate. The quality of the product streams can be defined in terms of the mole fraction of undesired and/or desired components in these streams. Process specific parameters such as recovery, purity can be suitably defined.

For determining the achievement of cyclic steady state by the system, the time averaged concentration in product tanks (such as raffinate and extract tanks) of each component over a cycle is compared with that over the previous cycle. In the present work, CSS is considered as achieved if the absolute difference between the two values for each component becomes less than or equal to a tolerance value of 10^{-4}. For rigorous quantification of numerical stability and convergence of the solution algorithm, apart from these gross convergence checks, mole balance check for each component is made for every cycle. At CSS, moles of ith component flowing into the bed over the entire cycle must be equal to the moles of that component flowing out from the bed. This should be true for all the components.

3. Simulation-based design

To begin with, simple adsorption breakthrough curves were simulated. In this, the bed was considered initially as devoid of any other adsorbate than the weakest adsorbate which is Methane. In other words, the adsorbent particles were considered as free of any adsorbed phase concentration. Feed was introduced in the bed at its pressure-composition-temperature conditions. Effluent specifications (13000-14000 SMCPH and content of less than or equal to 0.6% C_{2+} in raffinate) were observed. This was essential to get some feel of upper limit of adsorption step time in the eventual PSA cycle and also to gauge the amount of adsorbent requirement for specified capacity.

Desorption breakthrough of a fully saturated bed was also simulated by considering that the bed is purged with pure Methane (the weakest adsorbate) at the adsorption pressure and temperature to get an idea of the relative time scale of the regeneration time step duration. In actual cycle, purging step takes place with fraction of raffinate after the bed has been depressurized to the desorption pressure for systems where raffinate is the desired product such as this case.

These time steps would of course depend upon the adsorbent loading in the beds. Smaller the adsorbent loading, smaller would be the durations of both the steps.

These results with salient findings are presented below.

Typical adsorption breakthrough curves for a bed of 1.5 m diameter and 5 m height packed with 0.002 m spherical particles of Silica Gel adsorbent, 303.15 K temperature, 34 bara adsorption pressure and feed rate of 13800 SCMPH are shown in Figure 3 for Propane and

CO_2. The model predicts that Propane starts to come out of the bed from 515 seconds. Butanes will breakthrough later than Propane as they are adsorbed more strongly than Propane. So only the adsorption breakthrough behavior of Propane was followed out of the undesired alkanes (Propane and Butanes). The feed composition used and the isotherm parameters were as given earlier in Table 2. Mass transfer limitations were neglected due to the lack of data on the mass transfer coefficients. Initially the bed was assumed to be at the adsorption pressure of 34 bara and filled with pure CH_4 in both the phases. Adsorption breakthrough curve is a cycle having the step of only adsorption and desorption breakthrough curve is a cycle having the step of only desorption. Duration of these steps were entered for the respective cases. 15 divisions were used for the spatial discretization of the adsorbent layer and temporal step size was 1 second.
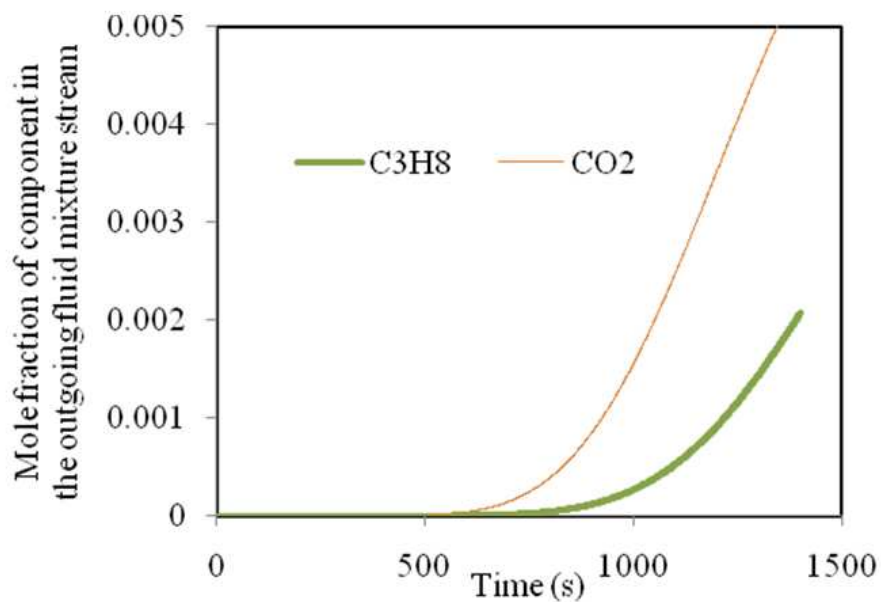

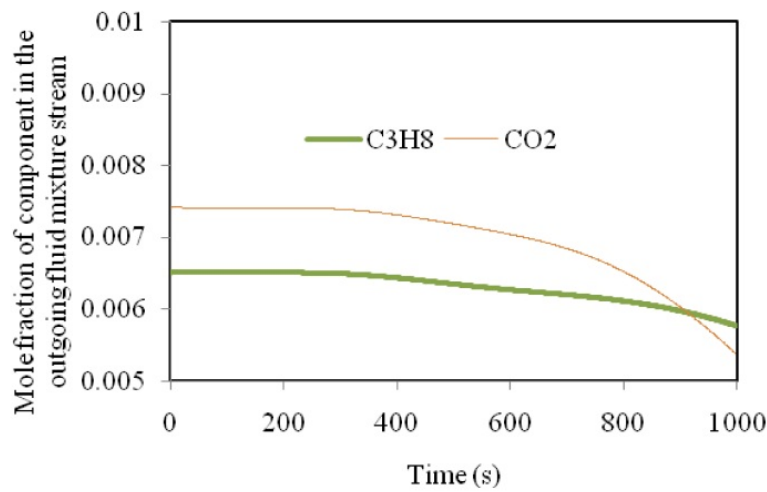**Figure 3.** Model predicted adsorption breakthrough curve for Propane and CO_2

It can be seen that even if the bed is fully regenerated each time before the adsorption step begins, the adsorption step time cannot be more than 1800 seconds if product stream has to have less than 0.1% of C_{2+}. More time can be kept if product stream can have more than this content of C_{2+}. These limits on concentration were for the mixed cup composition of the bed effluent stream, or raffinate. From this, the breakthrough concentrations had to be integrated along with the flow rates. The integrated concentration against time chart is also shown for this case in Table 6.

Desorption breakthrough curves are similarly presented in Figure 4. Initially the bed was assumed to be at the adsorption pressure of 34 bara and filled with the Natural Gas composition in the fluid phase. The solid phase composition of each component was in equilibrium with the fluid phase composition of that component. It was assumed that pure CH_4 was fed to this bed for 1000 seconds. The feed rate of this stream was kept nearly equal to the feed rate of Natural Gas mixture in the adsorption breakthrough curve simulation. The bed size, adsorbent, adsorbent dimensions, temperature used in the desorption

breakthrough and the feed rate of pure Methane were respectively same as that used in the adsorption breakthrough simulation. The stronger adsorbate (higher equilibrium constant) will require more time to be completely removed from the bed. This is observed in Figure 4 from the concentration profiles of Propane and Butanes.

Time (s)	% C_3H_8	% $n\text{-}C_4H_{10}$	%$i\text{-}C_4H_{10}$	% Total C_{2+}
2000	1.41E-01	1.54E-03	1.67E-04	1.43E-01
1800	9.96E-02	7.03E-04	6.36E-05	1.00E-01
1400	3.05E-02	7.78E-05	4.76E-06	3.06E-02
1200	1.15E-02	1.66E-05	8.29E-07	1.15E-02
1000	2.91E-03	2.32E-06	9.45E-08	2.91E-03

Table 6. Mixed-cup composition of raffinate against adsorption step time chart

(a)
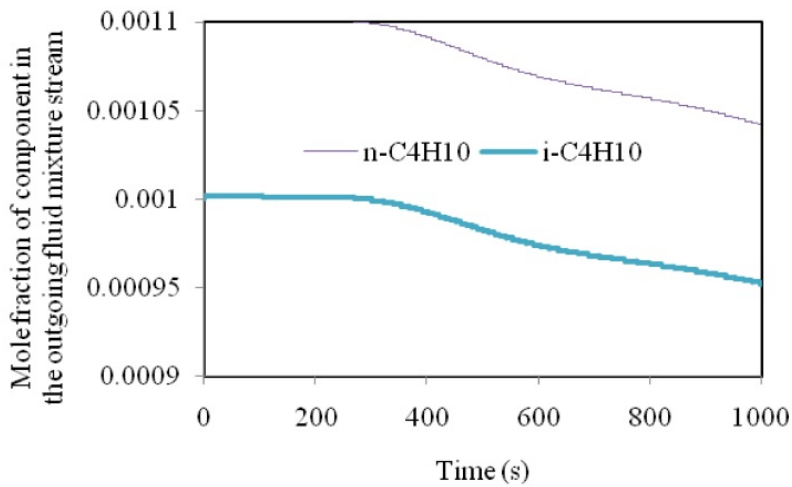
(b)

Figure 4. Model predicted desorption breakthrough curve for (a) Propane and CO_2 and (b) Butane isomers

In the actual PSA cycle, the regenerated bed is not entirely free of adsorbate and hence breakthrough would occur earlier. At the same time, during desorption, the bed is not initially fully saturated and desorption times could be smaller than observed above. The above adsorption-desorption comparison, nonetheless, gives an idea of two important steps of any PSA cycle, namely adsorption and regeneration. The total cycle time can be decided as follows. The feed rate and the purge rate are achieved by adjusting the raffinate valve and extract valve coefficient respectively. For a fixed feed rate, bed size and the valve coefficients, the time required to pressurize the bed from the desorption pressure to the adsorption pressure can be found by observing the model predicted pressure against time profile. Similarly, the time required to depressurize the bed back to the desorption pressure after the bed has completed the duration of the adsorption step can be found. The purge step duration can be tuned to get the desired purity. Thus the total cycle time can be obtained.

Most known PSA processes have matching adsorption and desorption step durations. Regeneration steps together must consume a total duration which is an integer multiple of total duration of adsorption steps [4]. If both the steps match in their durations, a 2 bed PSA system can be designed, with one bed in adsorption and one in desorption at any time. If desorption step is of a longer duration than adsorption duration, a 3 or 4 bed system can be conceived depending on whether the desorption time is twice or thrice of the adsorption time. 2 or 3 bed PSA systems are very common in this technology.

In the present case, the adsorption and desorption step times were of entirely different nature. The adsorption step was of much longer duration than the desorption. In fact, with the above initial simulations and more PSA simulations, it was seen that the range of adsorption-desorption steps is something like 600-100 seconds respectively. This would mean that the PSA system will have multiple beds, say 8, with 6 in adsorption step and 2 in desorption step at any time. These would further get fine tuned through simulations. However, it was apparent that an unconventional PSA cycle is in the offing.

The fact that we will need to have about 8 beds with 6 or 7 in adsorption step producing raffinate and 1 or 2 in desorption step producing extract, another important possibility emerged leading to the concept of surge-less PSA.

All known PSA plants use large drums as surge vessels. This is a necessity of PSA plants due to large surges in pressures and flows of raffinate and extract streams produced and feed used. The flow surges occur as a bed at low pressure is opened up to feed at high pressure and bed at high pressure is opened up to extract at lower pressure etc. At individual bed level, these pressure-flow surges an integral part of conventional PSA processes. Due to smaller number of beds employed, (2 or 3 bed cycles) these pressure surges also get transmitted to raffinate-extract-feed tanks. In the present case, as we anticipate to have 6 beds undergoing adsorption at various stages at any time, these beds produce raffinate streams at different flow rates and pressures simultaneously. The combined raffinate stream emerging from the beds undergoing adsorption is thus at a fairly uniform pressure and flow. There are pressure-flow surges during desorption as in the case

of any 2 or 3 bed PSA plants with 1 or 2 beds undergoing desorption simultaneously. If these could also be controlled in some way, the PSA process would operate as a surge-less process. This concept was pursued further giving rise to the surge-less PSA design.

Before we go to the actual design emerging out of the simulation studies, the operational advantage of a 12 bed PSA system with highly asymmetric durations of adsorption and desorption steps is presented in Figure 5 graphically. Each bed passes through the same step
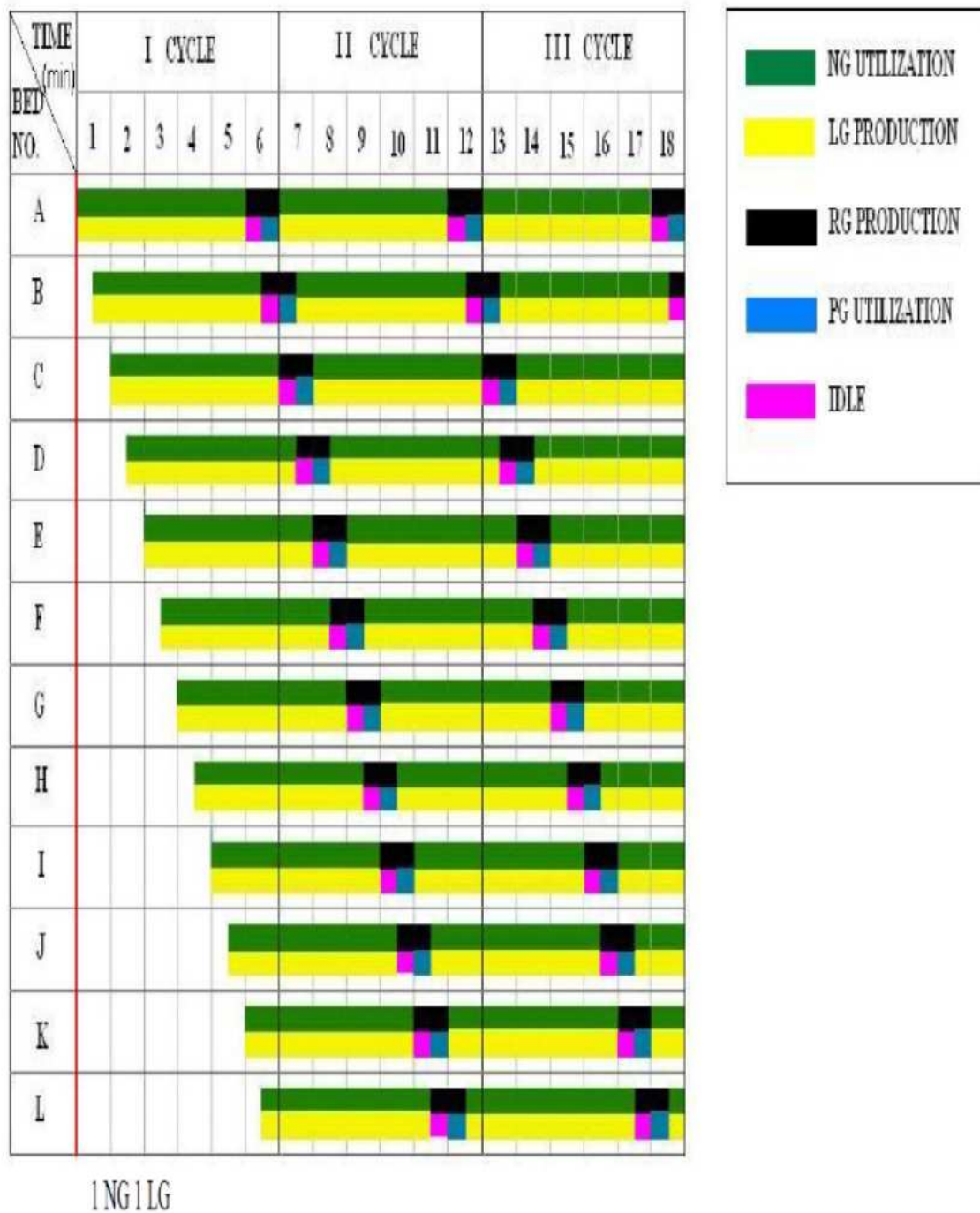

Figure 5. 12 bed system with t_cycle of 6 minutes and staggering time of ½ minute,(10 beds produce lean gas and 2 produce rich gas at any instant)

sequence. To get overall cyclic operation of the multi-bed system, the beds are staggered in their instants at which they start the first step of the PSA cycle. Staggering time is the total cycle time divided by the number of beds. Using the color code for the PSA steps as shown in Figure 5, the instantaneous position of the beds in this sequential execution of a PSA cycle employing 12 beds and a total cycle time of 360 seconds is summarized. The cycle described in this figure produces lean gas for 300 seconds and rich gas for 60 seconds. Natural Gas is fed for 300 seconds and the bed is purged for 30 seconds. The staggering time is 30 seconds. It can be seen that 10 beds are at various stages of saturation part of the PSA cycle while 2 beds are undergoing desorption/regeneration.

For the multiple-step cycle simulations, the feed composition, molecular weights or pure component and adsorption thermodynamics data was available as presented earlier in Table 2. The other required input data can be categorized as given by the captions of Tables 7-10. Feed gas had 98.4% of the desired components which are Methane and Ethane. If there are only ON/OFF valves, the flow rates to or from beds would depend on the instantaneous pressure differential available at the two ends of the valve. For example, at the start of a feed pressurization step, there is maximum pressure differential available and flow rates calculated using the valve equation could be very large. In actual practice also, the flow rates could be large causing the adsorbent bed to shake and cause undesirable attrition of particles. A control valve with appropriate time-adjusted valve opening could minimize these velocity surges. A 5-step PSA cycle having the steps of feed pressurization (10 seconds) + feed adsorption (560 seconds) + co-current depressurization(14 seconds) + counter-current depressurization (38 seconds) + purge (61 seconds) by fraction of raffinate was simulated on a column having 5 m adsorbent layer height. Two cases were studied. The first one had no controlled opening or closing of the valves unlike the valves for the second case. For the controlled case, instantaneous valve coefficient was given by Equation (10) as per linear valve characteristics. The value of valve coefficient at full opening (fo) or 100% opening (1st term in numerator of RHS of Equation (10)) is given for each valve in Table 10.

Sphericity	1
Particle diameter (mm)	2
Bed voidage	0.35
Inner Diameter of Bed (m)	1.5
Adsorbent Height (m)	5 (7 for lumping studies)
C_v of Feed Valve	0.01
C_v of Raffinate Valve	0.00029
C_v of Extract Valve	0.0038 (0.004 for lumped case)
C_v of Purge-in Valve	0.006

Table 7. Adsorbent, bed and valve properties used in the simulation

Adsorption temperature (K)	303.15
Feed Tank pressure (bara)	34
Raffinate Tank pressure (bara)	21
Extract Tank pressure (bara)	5.5
Purge-in Tank pressure (bara)	7.5
t_1 (s)	10
t_2 (s)	560
t_3 (s)	16
t_4 (s)	38
t_5 (s)	61
t_{cycle} (s)	685

Table 8. Operating conditions of the simulated cycle

Δz (m)	0.47
Δt for Step 1 (s)	0.10
Δt for Step 2 (s)	1.00
Δt for Step 3 (s)	0.10
Δt for Step 4 (s)	0.50
Δt for Step 5 (s)	1.00
Step size for Jacobian	0.001
Estimate of Euclidean distance of the solution from the initial estimate	100
Accuracy requirement	0.01
Max number of iterations	600000

Table 9. Numerical solver related data

Valve	C_v^{fo}
Feed	0.01
Raffinate	0.00029 (0.0003 for controlled opening and same feed rate as for no control case)
Purge-in	0.08
Extract	0.01 (0.00123 for controlled opening and same purge rate as for no control case)

Table 10. Coefficient at full opening of each valve

Time (s)	Raffinate valve	Purge-in valve	Feed valve	Extract valve
0	0	0	100	0
9.5	0	0	100	0
10	100	0	100	0
60	100	0	100	0
100	100	0	100	0
550	100	0	100	0
560	100	0	100	0
569.5	100	0	100	0
570	100	0	0	0
577	100	0	0	0
583.5	100	0	0	0
584	0	0	0	100
598	0	0	0	100
621.5	0	0	0	100
622	0	100	0	100
635	0	100	0	100
669	0	100	0	100
682.5	0	100	0	100
683	0	0	100	0

Table 11. % opening against time for each valve (No control)

Table 11 gives the percentage opening of each valve against time for the uncontrolled case. Table 12 gives a similar profile for the case of controlled opening and closing. In Table 11, it is seen that all the valves open at 100% opening immediately and completely close from full opening immediately. In Table 12, the feed valve opens with 10% opening and ramps up linearly to only 50% at the end of PF step. It ramps up linearly to 100% at the end of 60 seconds after the start of PF step. It starts to ramp-down from 550 seconds position to 60% at the end of 560 seconds and closes completely at the end of the adsorption step. Thus the ramp-up time of this valve is 60 seconds and ramp-down time is 20 seconds. The valve openings of the remaining three valves are as shown in Table 12. Again when a new cycle starts, it opens with 10% opening. Between 60 seconds to 550 seconds, it remains fully open. The percentage opening at intermediate time is found by interpolation. From the percent opening, the instantaneous coefficient of the valve is back-calculated as per valve characteristics say that given by the equation below. Equation (10) represents the characteristics of a linear opening valve and appropriate equation will have to be used if one has to use a control valve with other valve characteristics. The calculated valve coefficient is used in Equation (6) in the model equations.

$$C_V(t) = \frac{C_V^{fo}}{100} \% \text{Opening}(t) \tag{10}$$

The valve opening vs time profile is provided by the user as input to the simulation model. However, it can be deduced to begin with as follows. Consider the pressure of the bed after the end of PU step as P_5 and that of the feed gas as P_1. Let t_{PF} seconds be the duration of PF step. At the end of t_{PF} seconds, the pressure drop across the feed valve should ideally drop to zero from the starting value of (P_1-P_5).

Time (s)	Raffinate valve	Purge-in valve	Feed valve	Extract valve
0	0	0	10	0
9.5	0	0	45	0
10	10	0	50	0
60	100	0	100	0
100	100	0	100	0
550	100	0	100	0
560	100	0	60	0
569.5	100	0	10	0
570	100	0	0	0
577	100	0	0	0
583.5	10	0	0	0
584	0	0	0	1
598	0	0	0	100
621.5	0	0	0	100
622	0	10	0	100
635	0	100	0	100
669	0	100	0	100
682.5	0	10	0	10
683	0	0	10	0

Table 12. % opening against time for each valve (With control)

Even as the pressure drop across the feed valve drops with time, to get uniform draw of feed gas into the bed during this step, we should push same amount of gas every second into the bed. That is the velocity should be the same. Using Equation (6) and assuming constant flow velocity, we get Equation (11) which relates valve coefficients and pressures at two instances t_{1PF} and t_{2PF}. Valve Opening at (t_{2PF}) can be calculated using Equation (10).

$$\frac{C_V(t_{2PF})}{C_V(t_{1PF})} = \sqrt{\frac{(P_1\text{-}P(t_{1PF}))P(t_{2PF})}{(P_1\text{-}P(t_{2PF}))P(t_{1PF})}} \quad 0 \le t_{1PF} < t_{2PF} \le t_{PF}, P(t_{1PF}) < P(t_{2PF}) \le P_1 \quad (11)$$

Thus, if feed pressure (P_1) is 34 bara, bed pressure is 18 bara at time t_{1PF} [i.e. P_1 - $P(t_{1PF})$ = 16] and 30 bara at time t_{2PF} [i.e. P_1-$P(t_{2PF})$ = 4], the square root of pressure differential has only halved between the two time instants. If flow should be the same at both the instants, the C_V of feed valve at time t_{2PF} should be approximately thrice of its value at time t_{1PF}. If the feed valve characteristics are as per Equation (10), it would mean that its percentage opening at

time t_{2PF} should be also thrice of the percentage opening at time t_{1PF}. Same procedure can be applied for the remaining three valves to arrive at appropriate valve opening time series However, true surge-less operation will be achieved only if feed rate is ensured to be constant across pressurization and adsorption steps. Extract production rate is ensured to be constant across counter-current depressurization and purge steps. Raffinate production rate is ensured to be constant across adsorption and co-current depressurization steps and purge utilization rate is constant across purge step. This can be achieved only through percentage valve opening against time profile of control valves across each of the four valves.

Typical pressure and flow profiles at the two ends of any bed over a PSA cycle are shown in Figure 6 and Figure 7 respectively as given by the undashed lines for the case of controlled opening and closing and by the dashed lines for the case of uncontrolled opening and closing of the valves. There are significant surges in the velocity and the pressure for the case of uncontrolled opening and closing of the valves. However, the combined effect of all the beds together is much smoothened indicating the possibility of a surge-less PSA system or a PSA system with much smaller surge vessels. For operation with control, as seen from the undashed line in Figure 6, the bed has not reached the feed tank pressure, which it does after some duration of the adsorption step has elapsed. After that, the profiles are identical. In the depressurization step, controlled opening uses more time than the uncontrolled case to depressurize the bed to the desorption pressure value.

It is seen in Figure 7 that the superficial velocities for the case with no control have reached as high as 2.8 m/s in the pressurization step and then reach zero over half of its duration. It remains zero for the remaining half of the step. Comparatively the velocity variation for controlled opening case is less with the velocity magnitude not exceeding more than 1 m/s. Both the cases differ from each other in a similar manner in the depressurization step.
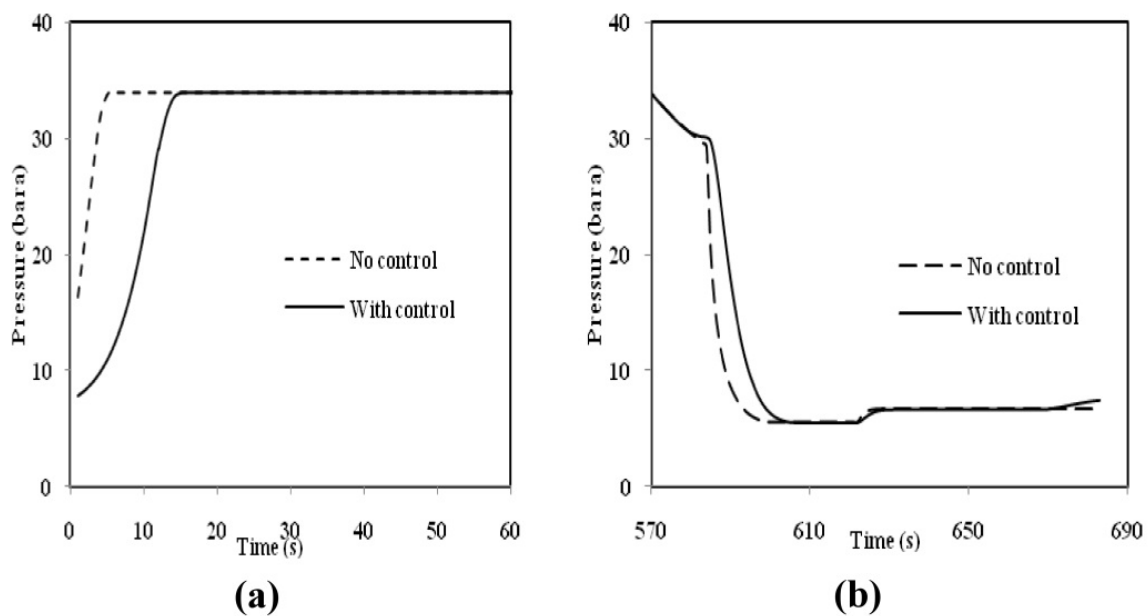

(a)   **(b)**

Figure 6. Pressure against time in (a) the feed pressurization step and the initial part of the feed adsorption step and (b) the depressurization steps and the purge step
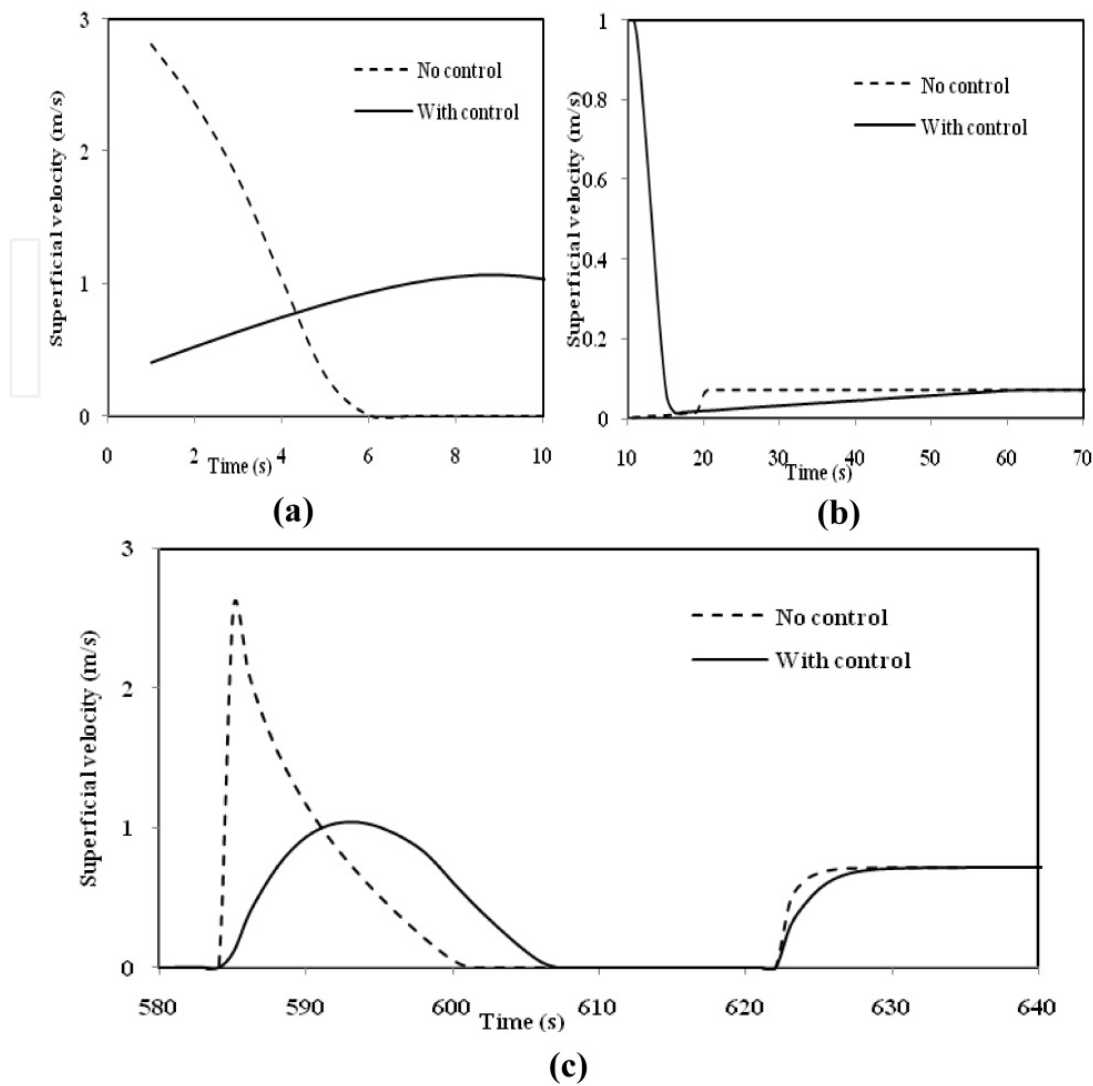
Figure 7. Superficial velocity against time for (a) the feed pressurization step, (b) first minute of the feed adsorption step and (c) the counter-current depressurization and the purge steps

Gradual pressurization is also preferred in kinetic separations like N_2-PSA [3]. Controlled opening is also better to prevent possible fluidization of the particles due to high velocity. Irrespective of whether the bed is getting pressurized or depressurized, controlled opening increases the time required to achieve the required pressure level, reduces the velocity variations and their magnitudes. It also helps to ensure that flow occurs during entire duration of the step smoothening the feed utilization or raffinate/extract production profiles.

Table 13 gives the comparison between the two cases based on important performance parameters. Separation performance is highly dependent on the purge rate or purge step duration. Using the same valve coefficients as that for the uncontrolled case, flow rates turned out to be lower for the first controlled case (middle column of Table 13). Since the purge rate is slightly lower for this controlled case, the purity is lower than that in the case where valve opening was not controlled (first column of Table 13). The last column in Table 13 gives the results for controlled case with feed rate and purge rates almost equal to that for

no control case. The flow rates were matched by increasing the coefficient for raffinate and extract valves at 100% opening respectively. This case gives higher purity than that for the case in second column. The purity increased because the purge rate was increased. Thus controlled opening and closing of the valve can also change the flow rates and the separation performance of the process. The purity for the second controlled case was lower than that for the uncontrolled case. Correspondingly, the recovery for the former case was higher.

	No control	With control-1	With control-2
Feed rate (SCMPH)	12544	12156	12532
Purge rate (SCMPH)	2385	2188	2391
CO_2+C_{2+} recovery %	71.4		72.9
C_1+C_2 % in raffinate (purity)	99.83	99.53	99.57

Table 13. Comparison of both the cases based on performance parameters

Although the multi-bed PSA plant was expected to give a reasonably surge-less operation, further reduction in surges was achieved by actually providing a control valve at product and feed ends of each bed and arriving at the time series of % opening of these valves over a PSA cycle.

It is thus possible to get a surge-less PSA with programmed control valves regulating feed and product flows during individual steps of a PSA cycle. The surge-less concept eliminated the need of surge tanks for the PSA plant bringing in major cost savings. The controlled opening and closing helps to reduce the magnitude of the velocity, reduce the velocity fluctuations and improves the utilization of the duration of depressurization and pressurization steps.
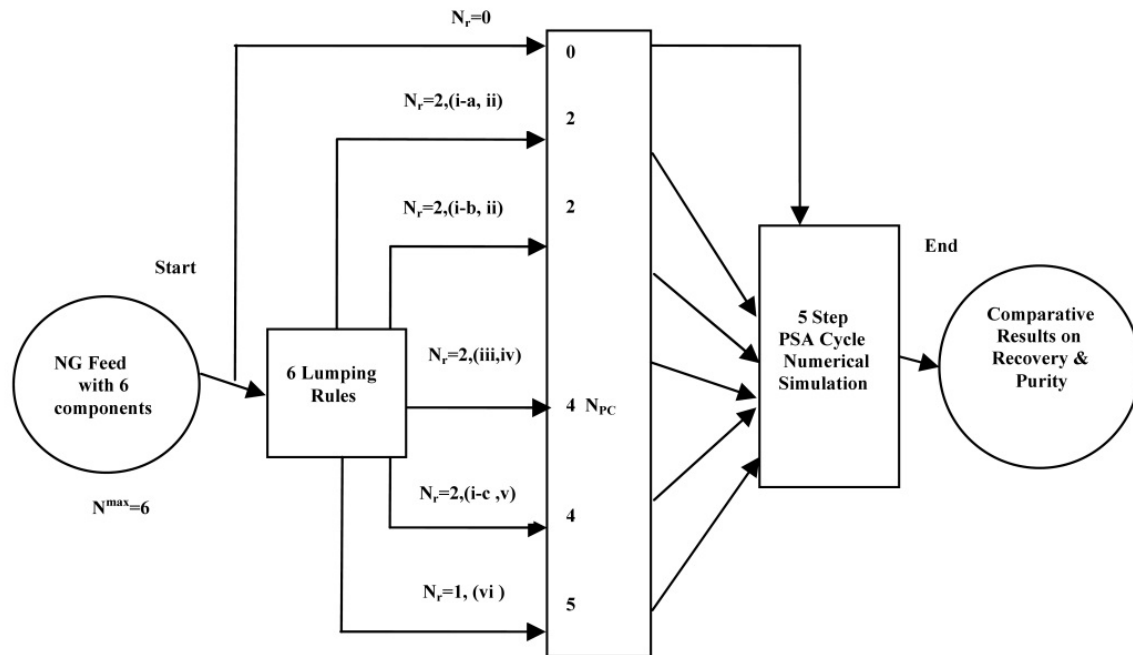
The multi-bed PSA plant also offered another advantage. The plant has been designed and commissioned in a plant environment where processing capacity varied as per downstream requirement. PSA cycles were designed to operate a total of 7, 6, 5, 4 and 3 beds only with reduced plant capacity so as to give same product purity and recovery. This allowed the plant to operate at a large range of turndown ratios unlike conventional 2-3 bed processes.

The simulation model is very rigorous and involves extremely heavy computational effort. Design is an iterative activity and would involve hundreds of such simulations. The scale of computations and array sizes depend upon the number of components. It was therefore considered desirable if some sort of component lumping could be considered in simulations such that the simulation results capture the salient performance appropriately. Once such lumped models indicate optimal design, a rigorous simulation could be carried out only for those cases or operation window around it. Without this, the simulation based design would have been impossible. This is briefly discussed in the next section.

4. Utility of component lumping in the cycle simulation

There is hardly any work on suitable lumping strategy for PSA cycle simulations. The authors carried out extensive work on developing such strategies. The lumping strategies

are covered in detail separately [5]. Mass transfer limitations were neglected due to lack of data of the mass transfer coefficients. Isotherm parameters of a pseudo-component are taken to be the weighted average of the isotherm parameters of all its member components. These and other properties such as molecular weights are given in Table 14. Lumping CH_4 with CO_2 or Ethane and heavier alkanes into a pseudo-component required modifying the definitions of the separation performance parameters. Salient features and relevant lumping for the present case are summarized below. A procedure to select the best strategy of component lumping is given in Figure 8. However before using the lumping strategy, care was taken to ensure that the step durations and bed dimensions were neither over-designed nor under-designed by observing the variable profiles for a case considering no lumping of components. Another point to be remembered is that in the simulations the number of components may get reduced by using various lumping rules, but to get the properties of the pseudo-components, the properties of each member component are required.

Lumping rules

(i)	Desired product is (i-a) C_1+C_2 or (i-b) C_1 or (i-c) C_1+CO_2	(iv)	Components have almost equal values of adsorption isotherm equilibrium constants
(ii)	Ratio of mole fraction of the desired product to the mole fraction of undesired or other components in the feed is greater than 15	(v)	Components have equal number of C atoms
(iii)	Components have equal values of molecular weights	(vi)	Keep distinct identity for inorganics, organic non-isomers having equal no. of C atoms and isomers

Figure 8. Flow-chart for the Lumping Strategy

Taking care of these two considerations, an extensive simulation program was launched. The bed height was increased to 7 m in these studies to keep a safety factor and the valve

coefficients are as given in Table 7. Lumping based simulations were done only for the uncontrolled case. The PSA cycle configuration is as per Table 8. The cases of lumping are given in Table 14 which gives the member components of a pseudo-component of a case and the simulation required properties of that pseudo-component. The computational and separation performances are summarized in Table 15 and Table 16. The impact of changing the feed composition, the operating temperature and the cycle configuration on the lumping strategy was also assessed. More details of these are given in our earlier published work [5]. Still the use of 2 pseudo-components with first one having Methane and Ethane as its member components and the second one having the remaining four components, predicted the separation performance closely with that predicted by using no pseudo-components (Case 1) with significant reduction in computation time and array sizes. Components of Natural Gas form a homologous series. However lumping strategy has to be used on a case to case basis.

Case	Pseudo-component	Member components	y_i	MW_i (kg/kmole)	b_i (m^3/mole)
2	1	C_1 and C_2	0.984	16.27	0.0006
	2	C_3, i-C_4, n-C_4 and CO_2	0.016	45.79	0.0089
3	1	C_1	0.9653	16	0.00055
	2	C_2, C_3, i-C_4, n-C_4 and CO_2	0.0347	37.22	0.006121
4	1	C_1	0.9654	16	0.00055
	2	C_2	0.0188	30	0.0025
	3	C_3 and CO_2	0.0138	44	0.007334
	4	n-C_4 and i-C_4	0.002	58	0.017233
5	1	C_1 and CO_2	0.9727	16.21	0.00067
	2	C_2	0.0188	30	0.0025
	3	C_3	0.0065	44	0.0084
	4	n-C_4 and i-C_4	0.002	58	0.017233
6	1	C_1	0.9653	16	0.00055
	2	C_2	0.0188	30	0.0025
	3	C_3	0.0065	44	0.0084
	4	n-C_4 and i-C_4	0.002	58	0.017233
	5	CO_2	0.0074	44	0.0064

Table 14. Member components and their properties for the lumped cases at 303.15 K

Compare results in Table 13 with results in Table 16. For the same feed valve coefficient, longer bed will require more time to get pressurized by the same pressure ratio. This implies that more flow will occur as the pressure drop across the valve remains higher than zero for a longer time in the longer bed. Apart from the adsorbent layer height, the purge-in and extract valve coefficients are lower in the cases considered for lumping studies compared to those used for getting the results in Table 13. So the average feed rate used in lumping

exercise (around 14000 SCMPH) was higher and the average purge rate (around 1600 SCMPH) was lower than the respective values used in comparing control valve approach with no control valve approach. As a result the separation performances differ. The purity has dropped to 99.4%. Velocity at the bed ends will depend on the pressure differential across the valve which will be higher for the longer bed. A longer bed will also require higher coefficient of the extract valve to depressurize it in the same duration and by the same pressure ratio. Else it will decrease the purity. The recovery has also dropped to 69%.

Case	Equations solved in adsorption step per call to solver	Range of CPU time (s) per cycle	Q^F (SCMPH)
1	218	313-332	13981
2	94	36-41	14034
3	94	44-79	13993
4	156	88-164	13984
5	156	88-164	14129
6	187	154-220	13983

Table 15. Equations, CPU time and feed rate for each case

Case	1	2	4	6
% moles of C_1+C_2 in Raffinate (Purity)	99.40	99.42	99.41	99.40
% Recovery of CO_2+C_{2+}	69.27	69.79	69.07	69.27

Table 16. Comparison of Case 2, Case 4 and Case 6 with Case 1

5. Conclusions

1. Pressure Swing Adsorption based process has been designed for the removal of Propane and higher alkanes from Natural Gas. The feed gas had six components and was available at a pressure as high as 34 bara. The raffinate requires to have as low content of Propane and higher alkanes as far as possible and come at a pressure higher than 20 bara for downstream use. The operating temperature was ambient value and the operating adsorption pressure was also equal to 34 bara. The adsorbent physically adsorbs the components in the following order: Butanes>Propane>Ethane>Methane. Natural Gas pre-treatment thus belongs to the type of raffinate PSA systems wherein the desired product is the weakly adsorbed component. Extended Langmuir adsorption isotherm parameters for each of the six components of the feed mixture were estimated from the pure component Langmuir isotherm data available in the literature.

2. A generic and rigorous mathematical model was developed to describe the discrete-continuous nature of the PSA cycle. This required solving large number of simultaneous non-linear algebraic equations numerically. The number of equations to be solved at any instant and the computational array sizes depend upon the number of components in the system. This is what makes the study of component-lumping

strategy in the cycle simulation worth considering for the purpose of reduction in computation time and array sizes.

3. The adsorption and desorption breakthrough curves were simulated using this model, actual feed mixture composition, industrial bed sizes and industrial flow rates. The starting duration of adsorption step in the cycle can be decided based on the adsorption breakthrough curve, predicted mixed cup composition of the impurity in the raffinate up to the chosen value of adsorption step duration and the allowable content of Propane and higher alkanes in the raffinate.

4. Like other raffinate PSA systems, this system also used the conventional four step Skarstrom cycle. Adding the step of co-current depressurization before the step of counter-current depressurization also helped to reduce the velocity variation during depressurization step by reducing the pressure difference. Thus a five step PSA cycle was able to give the desired separation performance with lesser velocity surges. As the amount of strongly adsorbed components were present in fraction less than 2% in the feed, the cycle did with 7 to 8 times higher adsorption step time than the desorption step time. The asymmetric distribution of the adsorption step duration and the desorption step duration is another distinguishing feature of this system. The separation performance and variable profiles for the case of uncontrolled opening were observed. Significant variations in velocity exist due to uncontrolled opening. The magnitude of velocity was also high for this case particularly during the initial instants of the pressure changing steps. The variable profiles were studied to ensure that the bed dimensions and the step durations are properly designed. These are to be ensured before the component-lumping strategy is used in the cycle simulation.

5. Then the cycle simulations were done using controlled opening and closing of the valves. Equations were derived to find the appropriate instantaneous opening of the valve required to get the desired pressure difference between the tank and the bed end at constant velocity in a given duration. The velocity and pressure profiles for the case of controlled opening and closing of valves were observed. This case showed significant reduction in the magnitude and variations in the velocity at the expense of more time being required to pressurize or depressurize the bed to the target pressure. The step duration was completely utilized for flow. Thus selecting appropriate step sequence in the cycle and controlling the valve opening/closing will help in minimizing the surge-tank costs and also improve the life of the adsorbent particles. The cycle used in this work uses more beds than in conventional 2-bed or 3-bed cycles. These beds operate in a staggered sequence and are able to ensure continuous feeding/production at any instant without needing surge tanks. A bed can be taken off-line for maintenance or due to reduction in product demand/feed gas availability. This allows flexibility in the capacity which is impossible in conventional 2-bed or 3-bed cycles.

6. To reduce the computation time and array sizes, up to six rules for lumping were applied. These enabled the use of as low as 2 pseudo-components to describe the original mixture of 6 components. The procedure to find the isotherm parameters and molecular weights of the pseudo-components was also developed. To find these, the respective properties of each member component are required. Separation performance

predicted by using the lumped case was compared with that predicted by using no lumping. The number of equations, computational times and array sizes were also compared and the lumped cases had significant savings in each of these against those of the non-lumped case. The feed mixture of 6 components was accurately described by a mixture of 2 pseudo-components where in Methane and Ethane are the members of the 1st pseudo-component and the remaining four components are the members of the 2nd pseudo-component. However, this strategy has to be applied on a case to case basis but is worth considering for multi-component mixture.

Nomenclature

b	Adsorption equilibrium constant of a component on the solid surface at the operating temperature, m^3/mole
c	Concentration of a component in the fluid phase, moles/m^3
C_v	Valve coefficient, unit-less
C_v^E	Coefficient of the extract valve, unit-less
C_v^F	Coefficient of the feed valve, unit-less
C_v^{fo}	Coefficient of the valve at 100 % (full) opening, unit-less
C_v^{max}	Maximum value from the valve coefficients, unit-less
C_v^{PI}	Coefficient of the purge-in valve, unit-less
C_v^R	Coefficient of the raffinate valve, unit-less
D	Inner diameter of the bed, m
d_P	Diameter of a spherical adsorbent particle or equivalent diameter for a non-spherical particle, m
g_c	Gravitational conversion factor, unit-less
i	Component index or Cycle step index, unit-less
j	Component index, unit-less
k^{LDF}	Coefficient of linear driving force approximation model for a component on the adsorbent, 1/s
L	Height of the adsorbent layer packed inside the column or spatial coordinate at the outlet of the bed in adsorption step, m
M	Number of divisions used for the spatial discretization of the adsorbent layer, unit-less
MW	Molecular weight of a component, kg/kmole
N	Number of components, unit-less
N^{max}	Maximum number of components considered in the feed mixture, unit-less
N_{PC}	Number of pseudo-components, unit-less
N_r	Number of lumping rules applied, unit-less

P	Absolute Pressure, Pa(a) or bara
P_1	Absolute pressure of Feed gas, Pa(a) or bara
P_5	Absolute Pressure at the end of purge step, Pa(a) or bara
P^{DS}	Pressure downstream of the valve, bara
P^E	Extract tank pressure, bara
P^F	Feed tank pressure, bara
P^{PI}	Purge-in tank pressure, bara
P^{RA}	Raffinate tank pressure, bara
P^{RI}	Pressure of the rinse-in tank, bara
P^{US}	Pressure upstream of the valve, bara
q^{max}	Maximum monolayer saturation capacity in the adsorption isotherm, moles /m^3 particles
Q^E	Volumetric flow rate of extract from the bed averaged over the duration of the extract production steps, SCMPH
Q^F	Volumetric flow rate of feed to the bed averaged over the adsorption step duration, NLPM or SLPM or NCMPH or SCMPH
q	Average concentration of a component adsorbed in the volume of adsorbent particles, moles/m^3 particles
q^{max}	Maximum monolayer adsorption capacity of a component on the adsorbent surface, moles/m^3 particles
q^*	Adsorption equilibrium concentration of a component in the solid phase, moles/m^3 particles
Q^{PI}	Volumetric flow rate of purge-in to the bed averaged over the duration of the purge step, SLPM or NLPM or SCMPH
Q^R	Volumetric flow rate of raffinate from the bed averaged over the duration of the raffinate production steps, SCMPH
R	Ideal Gas Law constant, Pa-m^3/mole/K
t	Time or Temporal coordinate, s
t_i	Duration of ith step of the cycle, s
t_{1PF}	An instant of the feed pressurization step, s
t_{2PF}	An instant of the feed pressurization step, s
T	Operating Temperature, K
t_{cycle}	Cycle time, s or minutes (1 minute = 60 seconds)
t_{PF}	Duration of feed pressurization step, s
u	Linear superficial velocity of the fluid, m/s
w	Mass fraction of a component, unit-less
y^{PI}	Fluid phase mole fraction of a component in the purge-in tank, unit-less
y	Fluid phase mole fraction of a component, unit-less
y^E	Fluid phase mole fraction of a component in the extract tank, unit-less

y^R	Fluid phase mole fraction of a component in the raffinate tank, unit-less
y^F	Fluid phase mole fraction of a component in the feed tank, unit-less
y_{UD}	Fluid phase mole fraction of the undesired product, dimensionless
z	Spatial coordinate, m
Δt	Size used for the temporal discretization of the duration of a step of the cycle, s
Δz	Size used for the spatial discretization of the adsorbent layer, m
ε	External voidage in the bed packed with the adsorbent particles, unit-less
μ	Dynamic Viscosity of the fluid mixture at the operating temperature, Pa-s
ϕ	Sphericity of the adsorbent or inert particle, unit-less
ϱ	Density of the fluid mixture at the operating conditions, kg/m^3
C_1	Methane
C_{1+}	Ethane and heavier hydrocarbons
C_2	Ethane
C_{2+}	Propane and heavier hydrocarbons
C_3	Propane
C_4	Normal Butane and Iso-Butane
CPU	Central Processing Unit
CSS	Cyclic steady state
DAE	Differential Algebraic Equation
i-C_4	Iso-Butane
LG	Lean Gas (Raffinate)
LPG	Liquified Petroleum Gas
n-C_4	Normal Butane
NG	Natural Gas (Feed)
PG	Purge-in Gas
RG	Rich Gas (Extract)
SCMPH	Cubic meters per hour at 273.15 K and 1 bara or 10^5 Pa absolute

Author details

Pramathesh R. Mhaskar and Arun S. Moharir[*]
Department of Chemical Engineering, IIT Bombay, Mumbai, India

6. References

[1] Daiminger U, Lind W, Mitariten M. Adsorption added value. Hydrocarbon Engineering 2006; 11(2) 83-86.

[*] Corresponding Author

[2]   Olivier M, Jadot R. Adsorption of Light Hydrocarbons and Carbon Dioxide on Silica Gel. Journal of Chemical and Engineering Data 1997; 42 (2) 230-233.

[3]   Mhaskar PR. Synthesis Strategies for Discrete-Continuous Adsorptive Separation Systems. PhD Thesis. IIT Bombay India; 2012.

[4]   Yang RT. Adsorbents: Fundamentals and Applications. John Wiley & Sons Inc. USA; 2003.

[5]   Mhaskar P, Moharir A. Multi-component Adsorptive Separation: Use of Lumping in PSA process simulation. Adsorption 2011; 17(4) 701-721.